

EXPERIMENTAL ANALYSIS OF TRANSVERSE STIFFNESS DISTRIBUTION OF HELICAL COMPRESSION SPRINGS

Robert BARAN^{*}, Krzysztof MICHALCZYK^{*}, Mariusz WARZECHA^{*}

^{*}Faculty of Mechanical Engineering and Robotics, Department of Machine Design and Maintenance, AGH University of Science and Technology, al. Mickiewicza 30, 30-059 Kraków, Poland

rbaran@agh.edu.pl, kmichal@agh.edu.pl, mwarzech@agh.edu.pl

received 27 September 2022, revised 13 December 2022, accepted 13 December 2022

Abstract: This paper presents the results of an experimental analysis of the distribution of transverse stiffness of cylindrical compression helical springs with selected values of geometric parameters. The influence of the number of active coils and the design of the end coils on the transverse stiffness distribution was investigated. Experimental tests were carried out for 18 sets of spring samples that differed in the number of active coils, end-coil design and spring index, and three measurements were taken per sample, at two values of static axial deflection. The transverse stiffnesses in the radial directions were tested at every 30° angle. A total of 1,296 measurements were taken, from which the transverse stiffness distributions were determined. It was shown that depending on the direction of deflection, the differences between the highest and lowest value of transverse stiffness of a given spring can exceed 25%. The experimental results were compared with the results of the formulas for transverse stiffness available in the literature. It was shown that in the case of springs with a small number of active coils, discrepancies between the average transverse stiffness of a given spring and the transverse stiffness calculated based on literature relations can reach several tens of percent. Analysis of the results of the tests carried out allowed conclusions to be drawn, making it possible to estimate the suitability of a given computational model for determining the transverse stiffness of a spring with given geometrical parameters.

Key words: helical spring, coil spring, transverse stiffness, end coils, stiffness distribution

1. INTRODUCTION

Cylindrical compression helical springs are widely used in mechanical systems as energy-storing components. Among the broad range of their applications, those requiring knowledge of the transverse stiffness of the spring pose immense challenges. Examples of such applications are vibratory conveyors [1], railroad bogies [2, 3], or vibration absorbers [4]. To support mechanical engineers in the design of such systems, many studies have been published in recent decades; mainly focusing on analytical models enabling the calculation of spring characteristics.

The published analytical models are generally based on simplifications and are therefore prone to errors. Yıldırım [5] reported differences between the results of the experiments and those obtained by elementary relationships for the static characteristics of cylindrical compression helical springs. Furthermore, Paredes [6] pointed out that the spring rate relationships available in the literature are characterised by sufficient accuracy only for springs with a coil number of not <5. The quoted work presented the results of experimental research on the axial compression of springs with two different ends (closed and ground ends and closed and not ground ends). Based on these results, a modification of the formulas for the number of active coils was proposed. Liu and Kim [7] analysed the effect of end coils on the natural frequencies of longitudinal vibration. They proposed a modification of the conventional analytical model in which the fixed boundary points at the ends of active coils were replaced by torsional stiffness elements, representing the end coils. The inclusion of end

coils in the calculations produced outcomes closer to the experimental results than the conventional model. The problem of transverse vibrations of cylindrical compression helical springs, which is of significant practical importance, was approached in many studies. Haringx [8] proposed a fundamental model of spring treated as an equivalent column, with the reference to the issue of its elastic stability and natural vibration frequencies. He assumed that spring has flat wound end coils with no contact with active coils. The model of the equivalent column was used by Wittrick [9] for the problem of spring vibration, including coupling between the longitudinal and torsional forms of vibration. The aforementioned coupling phenomenon was also considered in the work [10], in which the authors studied the wave phenomena occurring in a spring with a constant lead angle. The purpose of the work [11] was the unified dynamic analysis and dynamic criteria of stability for helical springs with the application of an equivalent beam model. Mottershead [12] proposed a new finite element modelling the coil or a part of a coil of a helical spring, whilst Taktak et al. [13] proposed a new finite element modelling the total behaviour of a helical spring. In all the cited works, the issue of the influence of end coils on transverse stiffness was neglected or subjected to only a partial analysis, as in paper [8]. The problem of the influence of passive coils on the frequency of transverse natural vibrations has been emphasised by Michalczyk [14] where, using numerical methods, significant discrepancies were shown between results obtained for springs differing in the end-coils shape. The same phenomenon was demonstrated experimentally by Michalczyk and Bera [15]. This influence is mainly related to the elastic susceptibility of passive coils.

To ensure the stable operation of cylindrical compression helical springs, their ends should be closed and ground – this is form D according to ISO 2162-2:1993. For durability reasons, the EN13298:2003 standard specifies that the extremity of each end coil should have, after the grinding, a thickness between 3 mm and one-quarter of the wire cross-section. In extreme cases, the contact line between the end coil and the adjacent active coil can take the form of a point. In this case, the concentration of contact stresses and wire abrasion have a negative effect on the fatigue strength of the spring [16]. Increasing the contact length between the end and active coils has a positive effect on contact stresses but at the same time increases the mounting space of the spring.

Effects related to the length of the contact line between the end coils and adjacent active coils are neglected in the models currently used to calculate the transverse stiffness of cylindrical compression helical springs. The transverse stiffness values determined on their basis have a uniform distribution in all directions perpendicular to the spring axis. The problem of nonuniformity of stiffness distribution in the direction perpendicular to the spring axis is important in suspension systems of vibrating machines and rail vehicles. The springs are placed in holders in the appropriate position to eliminate the differences in transverse stiffness and eccentricity in the transmission of axial force. Any positioning of the springs in relation to each other could cause an uneven distribution of vibrations, manifesting itself in driving discomfort, or even damage to the suspension by spring failure, usually in the area of the end coil [17]. In addition, in the case of sets of coaxially aligned springs, there is a risk of collision between the inner and outer springs. This phenomenon is especially dangerous for those springs, especially the inner one, which is the most loaded [18].

Despite the extensive literature on the static and dynamic properties of helical springs, the impact of the shape of the end coil on these properties has not been fully explained. The significance of this impact increases with the decreasing number of active coils.

This paper aims to investigate the effect of contact line length between end coils and adjacent active coils and the number of active coils on the transverse stiffness distribution of springs, and to investigate the relationship between experimental results and those of known computational models from the literature. This will improve the cylindrical compression helical spring design process for applications where transverse stiffness is an important aspect. The experimental results presented in this paper, together with a description of the geometry of the springs tested, can also provide a benchmark for validating numerical models of springs.

2. METHODOLOGY

2.1. Sample selection – geometrical and material properties

To carry out the tests, springs with parameters determined by a strict mathematical model were designed. Each spring has end coils on both sides with the same pitch as the wire diameter, and active coils in the middle part with a determined working pitch. The spring wire axis is rounded with a fixed radius at the pitch change point. Each of these spring sections was described by mathematical equations and then a path was generated using the Python programming language to represent the spring wire axis. To examine the influence of the contact line length on the stiffness

distributions, three forms of end coils were designed as shown in Fig. 1.

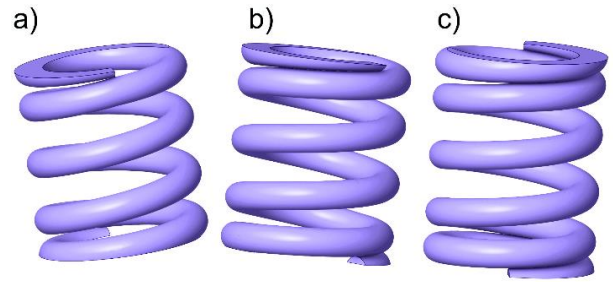


Fig. 1. Closed and ground end coil with (a) point contact with active coils, (b) with contact at 0.25 of coil length and (c) with contact at 0.5 of coil length

Fig. 1a shows a spring with point contact between passive and active coils. The number of passive coils of this spring is 2. Fig. 1b presents a model of a spring for which the contact line length between coils on each side equals 0.25 of a coil and the number of passive coils equals 2.5. Fig. 1c presents a spring with contact line length of 0.5 of a coil on each side and the number of passive coils equals 3. For the sake of simplicity, in the following part of the paper, the forms of end coils shown in Fig. 1a will be denoted as e1, the forms shown in Fig. 1b will be denoted as e2, and the forms shown in Fig. 1c will be denoted as e3. The pitch of the spring in the active area in the unloaded condition was 10 mm for all springs. As mentioned above, a lower number of active coils increases the influence of end coils on the static characteristics of cylindrical compression helical springs. Considering this fact and taking into account the design space of various applications, three different numbers n_a of active coils were selected for analysis: 2.5, 2.75 and 3. Moreover, two different spring indexes C were considered: 5 and 7.

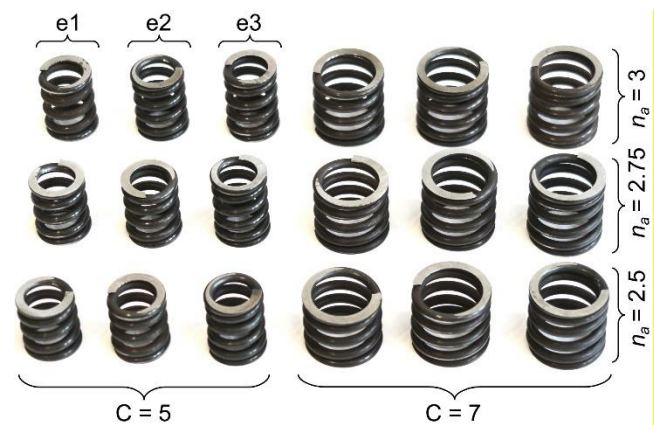


Fig. 1. Single samples intended for laboratory research

Tab. 1. Parameters of spring samples selected for experimental testing

Active coils	$n_a = 2.5$			$n_a = 2.75$			$n_a = 3$			
End-coil shape	e1	e2	e3	e1	e2	e3	e1	e2	e3	
Spring index C	5	7	5	7	5	7	5	7	5	7

The springs used in the experiments were manufactured by a supplier under the EN 13906-1:2013 standard. All springs were coiled from wire with a diameter $d_w = 5$ mm made of 55CrSi FD Becrosi 26 spring steel, which complies with the EN-10270-2 standard. The modulus of elasticity in tension E and the modulus of elasticity in shear G for this material were 206 GPa and 79.5 GPa, respectively. After winding, the springs were tempered at 220°C for 15 minutes, then the end coils were ground to $\frac{3}{4}$ of the circumference and subjected again to the same heat treatment. All 18 combinations of the spring parameters listed above are shown in Tab. 1. Fig. 2 shows a set of 18 spring samples to be tested with the parameters listed in Tab. 1.

2.2. Test setting

The tests were carried out using an HT-2402 testing machine from Hung Ta Instrument Co., Ltd., Taiwan, equipped with a CL16md 5kN load cell from ZEPWN, Poland, of the precision class 0.5 according to ISO 376 (Fig. 3a).

To measure the transverse stiffness of a spring, the spring must be preloaded before applying a force perpendicular to its axis. To enable such measurements, an adapter device was designed and built (Fig. 3b). The adapter was made based on 45 mm x 45 mm strut profiles with high axial and flexural stiffness. Its design minimises the loads transferred from the tested springs to its components, so the elastic deformation of the adapter is negligibly small compared to that of the tested springs.

To achieve axial preload of spring 1, the distance between brackets 2 and 3 was adjusted by moving bracket 2 with the help of a screw fitted with knob 6. Once the correct axial spring compression was achieved, measured using a digital caliper, bracket 2 was fixed. The force transverse to the axis of the spring was applied by pressing the head of the testing machine against rail 4 in the direction indicated by the red arrow in Fig. 3b. Rail 4 was assembled to the HIWIN HGW15CC linear guideway 5.

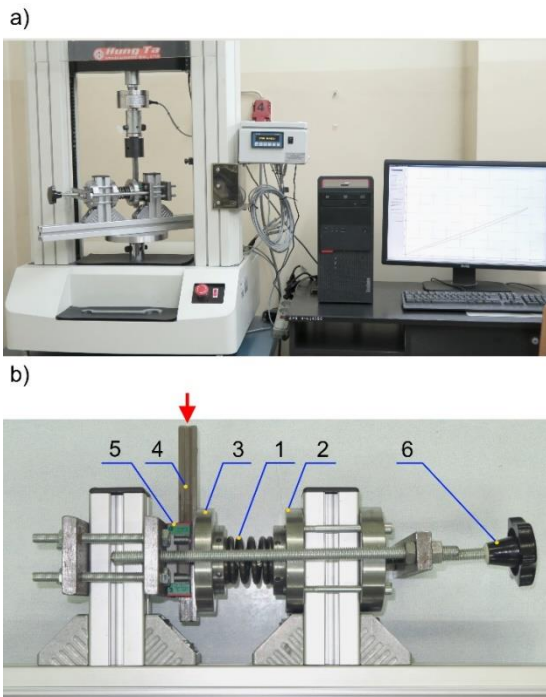


Fig. 3. The test stand (a) and adapter (b) for measuring transverse stiffness

A similar design solution for a fatigue test bench for railway springs is presented in paper [19], while paper [20] describes a bench that only allows the axial stiffness testing of the springs.

The pretension force applied to the spring causes motion resistance in the linear guideway of the adapter. This resistance results in forces which can influence measurements of the spring transverse stiffness. To assess whether those forces are significant or can simply be omitted, additional tests were performed. For those tests, the adapter device was modified. The main modification was the inclusion of a second, identical linear bearing. Therefore, during the tests, the motion resistance of both linear bearings was measured simultaneously. The tests were carried out at spring pretension nominal values of 125 N, 250 N, 500 N, 750 N and 1,000 N, which approximately covers the entire range of loads acting on the linear bearing during the tests of their transverse stiffness. Fig. 4a shows the registered resistance force values for an exemplary test with a pretension force equal to 1,000 N. The tests consisted of forcing both guides to move by a value of 10 mm with a rate of 6 mm/min and recording the resistance force. Each test was repeated five times for a given load value. The obtained results allowed the calculation of the average linear bearing resistance force as shown in Fig. 4b. The largest average drag force of two linear bearings did not exceed 9 N. Due to the small values of the resistance forces of a single linear bearing, these forces were omitted from the calculations.

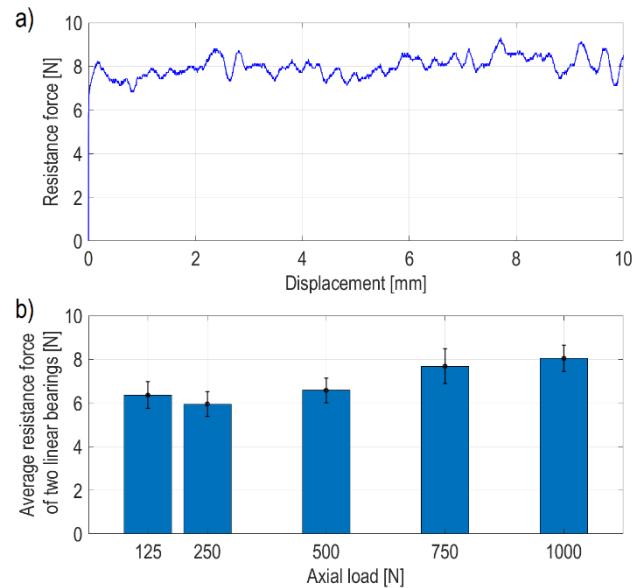


Fig. 4. Example record: (a) variation of the resistance force as a function of bearing displacement, with an axial load of 1,000 N; (b) average resistance forces of two linear bearings for five different axial loads

2.3. Transverse stiffness tests

Transverse stiffness measurements were carried out on axially compressed springs. The value of axial compression corresponded to 25% (denoted as c25) and 50% (denoted as c50) of the total clearance between the active coils. This way of achieving the axial load made it possible to apply a proportional load to each spring and therefore enabled a comparison of the results obtained. The transverse deflection was selected so that the maximum tangential stress did not exceed the value of 50% of ultimate

stress in the worst case. The second condition for the selection of the transverse deflection is the condition of stability, necessary for the spring ends resting on their supports. This condition is formulated in the EN 13906-1:2013 (E) standard:

$$F_Q \cdot \frac{L}{2} \leq F_0 \cdot \frac{D-s_Q}{2} \quad (1)$$

where: F_0 is the axial force, F_Q is the lateral force, L is the total spring length, D represents the nominal spring diameter and s_Q is the transverse deflection. As a result of trial calculations, it was assumed that the maximum transverse displacement of the moving end of the spring during the experiment would be 0.0933 of the axial deflection. The axial deflection values and the corresponding transverse deflection values are presented in Tab. 2.

Tab. 1. The values of transverse deflections for each number of active coils and the value of axial deflections

Active coils	$n_a = 2.5$	$n_a = 2.75$	$n_a = 3$
Axial deflection [mm] (c25)	3.13	3.44	3.75
Transverse deflection [mm] (c25)	2.04	2.25	2.45
Axial deflection [mm] (c50)	6.25	6.88	7.50
Transverse deflection [mm] (c50)	1.75	1.92	2.10

For each spring, at the given preload, 12 measurements were made by changing the direction of the transverse load. To achieve this, the tested spring was rotated with respect to the test stand with angular increments of 30°. Each measurement at a fixed angle value was repeated three times, and then the average value from these measurements was calculated. The arrangement of load directions and spring geometry is presented in Fig. 5.

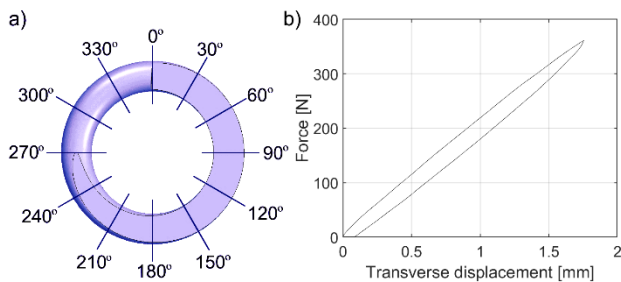


Fig. 2. An angular coordinate system (a) defining transverse load directions in subsequent tests of transverse stiffness for a single spring (view from the sliding support side) and (b) sample test record for measuring the transverse stiffness of a spring

The transverse stiffness was determined as the quotient of the maximum transverse force to the corresponding maximum deflection. Although inequality Eq. (1) was satisfied for all the experimental conditions shown in Tab. 2, some springs in the tests at c25 axial deflection lost stability at certain angular positions before reaching the maximum assumed value of lateral deflection. In these cases, the stiffness was determined from the stable part of the characteristic. The total number of transverse stiffness measurements taken was 1,296.

3. RESULTS AND DISCUSSION

3.1. Results of the Experiments

The transverse stiffness distributions as a function of the direction of the transverse force (see Fig. 5a) obtained based on the experiments under axial deflection c50 are shown in Figs. 6–8. The transverse stiffness at individual points in those figures is average values with standard deviation for three measurements of each spring. The results are repeatable because the coefficient of variation for each measurement point did not exceed 2%. This shows sufficient accuracy in measuring transverse stiffness with the use of the designed stand, which means the possibility of concluding based on these tests. Fig. 6 shows the transverse stiffness distribution for springs with $n_a = 2.5$, Fig. 7 shows the transverse stiffness distribution for springs with $n_a = 2.75$ and Fig. 8 shows the analogical plots for springs with $n_a = 3$.

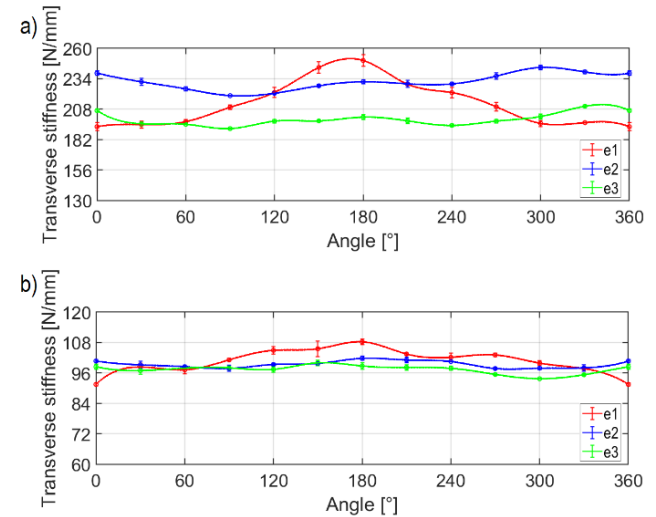


Fig. 6. Transverse stiffness distribution for springs with $n_a = 2.5$, and spring index (a) $C = 5$ and (b) $C = 7$

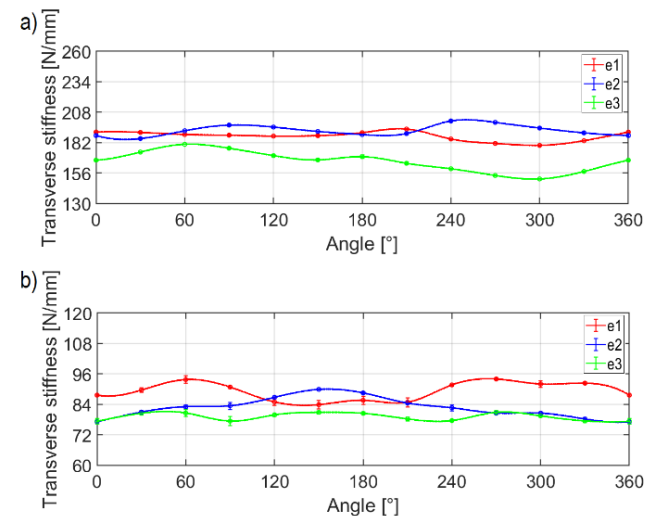


Fig. 7. Transverse stiffness distribution for springs with $n_a = 2.75$, and spring index (a) $C = 5$ and (b) $C = 7$

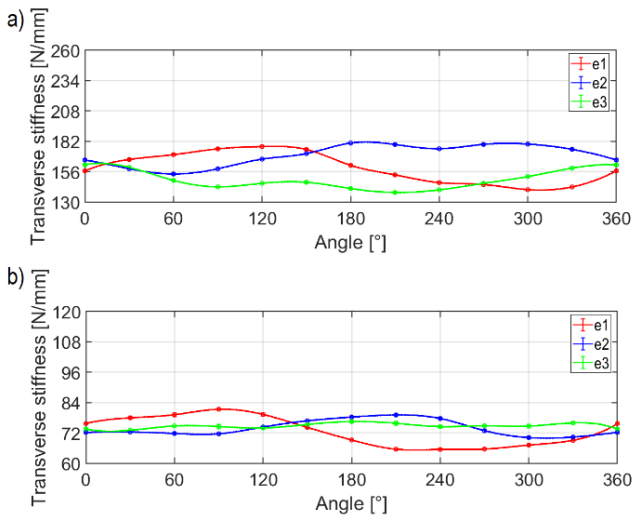


Fig. 8. Transverse stiffness distribution for springs with $n_a = 3$, and spring index (a) $C = 5$ and (b) $C = 7$

As is evident from Figs. 6–8, the transverse stiffness was significantly dependent on the direction of the applied force. This phenomenon is a consequence of changes in the geometry of the spring’s end coils and their mutual positioning.

The measurement data presented in Figs. 6–8 revealed the influence of the design of the end coils of the spring on its transverse stiffness. It can be seen that increasing the number of passive coils from e1 to e3 is not necessarily accompanied by a reduction in spring transverse stiffness.

For a more precise comparison of the results obtained, their statistical parameters were calculated (Tabs. 3 and 4). They allow the variability of the stiffness distribution on the circumference of the spring to be assessed and to indicate the influence of the shape of the end coils, the partial number of active coils and the spring index on this distribution. The relative gap that occurs in the last column in Tabs. 3 and 4 is calculated as the gap between the maximum and minimum stiffness values in the entire 360° range divided by the mean stiffness value. The coefficient of variation shown in Tabs. 3 and 4 relates to the variation of the stiffness distribution as a function of load angle.

Tab. 3. Statistical analysis of transverse stiffness distribution for the c25 axial load

Spring index C	Number of active coils n_a	End-coil shape	Mean transverse stiffness [N/mm]	Coefficient of variation [%]	Maximum value N/mm (angle of occurrence)	Minimum value N/mm (angle of occurrence)	Relative gap [%]
5	2.5	e1	164	3.8	175/0°	153/300°	13.7
		e2	186	5.0	209/0°	170/270°	21.5
		e3	163	4.1	176/210°	153/120°	14.4
5	2.75	e1	154	7.4	171/60°	136/150°	22.7
		e2	160	3.5	170/150°	151/240°	11.9
		e3	137	3.5	148/150°	132/270°	11.7
5	3	e1	127	4.6	138/120°	118/30°	16.3
		e2	142	5.6	154/180°	130/60°	17.2
		e3	125	1.5	128/330°	121/300°	5.4

7	2.5	e1	84	3.2	87/90°	78/270°	11.3
		e2	85	4.9	91/60°	78/300°	14.8
		e3	80	6.6	92/210°	70/300°	26.7
7	2.75	e1	78	7.7	88/60°	71/150°	21.5
		e2	75	4.5	83/150°	72/30°	14.6
		e3	69	4.5	74/60°	64/180°	13.3
7	3	e1	71	2.1	73/30°	68/300°	6.8
		e2	66	3.2	68/300°	61/0°	12.0
		e3	67	2.4	69/180°	64/240°	7.6

Tab. 2. Statistical analysis of transverse stiffness distribution for the c50 axial load

Spring index C	Number of active coils n_a	End-coil shape	Mean transverse stiffness [N/mm]	Coefficient of variation [%]	Maximum value N/mm (angle of occurrence)	Minimum value N/mm (angle of occurrence)	Relative gap [%]
5	2.5	e1	214	9.2	250/180°	193/0°	26.5
		e2	231	3.2	244/300°	220/90°	10.4
		e3	199	2.7	210/330°	191/90°	9.6
5	2.75	e1	187	2.2	194/210°	180/300°	7.4
		e2	193	2.4	200/240°	185/30°	7.8
		e3	166	5.5	181/60°	151/300°	17.8
5	3	e1	159	8.6	177/120°	141/300°	23.2
		e2	170	5.5	180/180°	154/60°	15.5
		e3	149	5.3	162/0°	138/210°	15.9
7	2.5	e1	101	4.5	108/180°	91/0°	16.6
		e2	99	1.4	102/180°	98/270°	4.0
		e3	97	1.8	100/150°	94/300°	6.4
7	2.75	e1	89	4.2	94/270°	84/150°	11.3
		e2	83	4.7	90/150°	77/0°	15.4
		e3	79	1.9	81/270°	77/0°	4.4
7	3	e1	72	8.4	81/90°	65/240°	21.9
		e2	74	4.3	79/210°	70/300°	12.1
		e3	75	1.3	76/180°	73/30°	4.6

By analysing the results in Tabs. 3 and 4, it can be seen that both at axial deflection c25 and c50, the differences between the maximum and minimum values of transverse stiffness for a single spring can exceed 25% of its average stiffness. Axial deflection significantly affects the stiffness distribution as it changes the partial number of active coils. This can be seen in the example of a spring with index $C = 7$, $n_a = 2.5$ and end-coil shape e3, for which the relative gap is 26.7% at axial deflection c25 and at axial deflection c50 the relative gap is only 6.4%. The calculation of the coefficient of variation showed that the variability of the transverse stiffness distribution on the circumference of the spring does not exceed 10% for the geometric and measurement parameters adopted.

In the case of springs with index $C = 7$, no significant effect of end-coil design on stiffness was observed, while in the case of springs with $C = 5$, the effect is distinct. The springs with index C

= 5 and the end-coil design e2 showed significantly higher stiffness than the springs with the end-coil shapes e1 and e3.

Analysing the angular coordinates of the occurrence of maximum and minimum stiffnesses, no clear trend can be observed regarding the influence of geometrical parameters. This is because each deflection closes a different number of active coils, which translates into a different stiffness for individual directions of the transverse load.

3.2. Analysis of results and comparison with results of analytical formulas

The measurement data presented in Section 3.1 showed a relatively large variation in the transverse stiffness with the change in the direction of the load force. By contrast, the analytical equations available in the literature assume a constant value of transverse stiffness R_Q . To confront those values with the measurement data, the most renowned analytical formulas of Gross, Wahl, and Haringx (the latter used in the EN 13906-1:2013 standard) were selected. These formulas are presented below. Transverse stiffness according to Gross [21]:

$$R_Q = \frac{1}{\frac{1}{F_0} \left[\frac{2}{\alpha \sqrt{1 - \frac{F_0}{\beta}}} \tan \left(\frac{h}{2} \sqrt{\frac{F_0}{\alpha(1 - \frac{F_0}{\beta})}} \right) - h \right] + \frac{h}{\beta}} \quad (2)$$

where: F_0 is the axial force, h is the length of the loaded spring.

The quantities α and β are the bending and shearing stiffnesses, respectively:

$$\alpha = \frac{2 \cdot h \cdot J \cdot E \cdot G}{\pi \cdot n \cdot \alpha \cdot \frac{D}{2} \cdot (2G + E)} \quad (3)$$

$$\beta = \frac{E \cdot h \cdot J}{\pi \cdot n \cdot \alpha \cdot \left(\frac{D}{2}\right)^3} \quad (4)$$

In Eqs (3) and (4), E represents Young's modulus, G is the shear modulus, J is the second moment of the cross-section area of the wire, and D is the nominal diameter of the spring.

Below, the Wahl [22] method is presented:

$$R_Q = \left(1 - \frac{2 \cdot F_0}{\beta \left(\sqrt{1 + \frac{4 \cdot \pi^2 \cdot \alpha}{h^2 \cdot \beta}} - 1 \right)} \right) \cdot \left(\frac{h^3}{12 \cdot \alpha} + \frac{h}{\beta} \right)^{-1} \quad (5)$$

Calculation by Haringx [8]:

$$R_Q = \frac{F_0}{h \left(\frac{1 + \frac{F_0}{\beta}}{\frac{1}{2} h \sqrt{\frac{F_0}{\alpha} \left(1 + \frac{F_0}{\beta} \right)}} - 1 \right)} \quad (6)$$

The computational model proposed by Haringx [8] was used in the transverse stiffness calculation method presented in the EN 13906-1:2013 standard. The calculation formulas in this standard can be presented in the following form:

$$R_Q = \frac{\gamma}{h} \cdot \eta \quad (7)$$

where:

$$\eta = \xi \left[\xi - 1 + \frac{\frac{1}{\lambda}}{\frac{1}{2} + \frac{G}{E}} \cdot \sqrt{\left(\frac{1}{2} + \frac{G}{E} \right) \left(\frac{G}{E} + \frac{1 - \xi}{\xi} \right)} \cdot \tan \left(\lambda \cdot \xi \cdot \sqrt{\left(\frac{1}{2} + \frac{G}{E} \right) \left(\frac{G}{E} + \frac{1 - \xi}{\xi} \right)} \right) \right]^{-1} \quad (8)$$

$$\gamma = \frac{G \cdot h \cdot J}{\pi \cdot n \cdot \alpha \cdot \left(\frac{D}{2}\right)^3} \quad (9)$$

where ξ represents the relative axial deflection of the spring, λ is the spring slenderness defined as a quotient of a spring free length to its mean diameter, and γ represents the compression stiffness of the spring.

Since the EN 13906-1:2013 standard uses the Haringx model, the results obtained using Eq. (7) are the same as the results obtained using Eq. (6). The results based on Eqs (8) and (9) were compared with the values measured during the tests. The experimental results were averaged and given statistical parameters. The results obtained for the axial load c25 are presented in Tab. 5 and for the axial load c50 in Tab. 6. For each stiffness value calculated based on a given method, the relative change between the experimental result and the result of this method is given in parentheses.

As shown in Tabs. 5 and 6, analytical methods generally underestimate stiffness values, especially for springs with index $C = 5$. The comparison presented demonstrated that analytical relations give only approximate values of the spring transverse stiffness, which may not be sufficient for precise designs. Moreover, they give different values, leaving the designer with the problem of choosing one of them.

Tab. 3. Comparison of the mean values of the measured transverse stiffness (for c25 axial deflection) and their deviations from the calculations by analytical methods

Spring index C	Number of active coils n_a	End-coil shape	Mean transverse stiffness [N/mm]	Gross method [N/mm]	Wahl method [N/mm]	Haringx method [N/mm] (and PN EN 13906:2013)
5	2.5	e1	164	190 (16%)	163 (0%)	186 (14%)
		e2	186	174 (-7%)	150 (-19%)	170 (-9%)
		e3	163	158 (-3%)	138 (-15%)	155 (-5%)
5	2.75	e1	154	159 (3%)	135 (-12%)	155 (1%)
		e2	160	145 (-10%)	124 (-22%)	141 (-12%)
		e3	137	132 (-4%)	115 (-16%)	129 (-6%)
5	3	e1	127	133 (5%)	113 (-11%)	130 (2%)
		e2	142	122 (-14%)	104 (-27%)	119 (-16%)
		e3	125	111 (-11%)	96 (-23%)	109 (-13%)
7	2.5	e1	84	95 (14%)	93 (11%)	94 (12%)

		e2	85	89 (6%)	87 (3%)	88 (4%)
		e3	80	84 (5%)	82 (3%)	83 (4%)
		7	2.75	e1	78	82 (5%)
		e2	75	77 (2%)	75 (-1%)	75 (0%)
		e3	69	72 (4%)	70 (2%)	71 (3%)
		7	3	e1	71	71 (0%)
		e2	66	66 (0%)	64 (-2%)	65 (-1%)
		e3	67	62 (-7%)	60 (-10%)	61 (-9%)

7	3	e1	72	75 (3%)	71 (-3%)	72 (0%)
		e2	74	70 (-5%)	66 (-11%)	62 (-17%)
		e3	75	66 (-12%)	62 (-17%)	63 (-15%)

Tab. 4. Comparison of the mean values of the measured transverse stiffness (for the c50 axial deflection) and their deviations from the calculations using analytical methods

Spring index C	Number of active coils n_a	End-coil shape	Mean transverse stiffness [N/mm]	Gross method [N/mm]	Wahl method [N/mm]	Haringx method [N/mm] (and PN EN 13906:2013)
5	2.5	e1	214	202 (-5%)	190 (-11%)	194 (-9%)
		e2	231	184 (-21%)	172 (-25%)	176 (-24%)
		e3	199	167 (-16%)	157 (-21%)	160 (-20%)
5	2.75	e1	187	169 (-10%)	158 (-16%)	162 (-14%)
		e2	193	153 (-21%)	143 (-26%)	146 (-24%)
		e3	166	139 (-16%)	130 (-22%)	133 (-20%)
5	3	e1	159	142 (-11%)	132 (-17%)	135 (-15%)
		e2	170	128 (-25%)	120 (-30%)	122 (-28%)
		e3	149	116 (-22%)	108 (-27%)	111 (-25%)
7	2.5	e1	101	100 (-1%)	95 (-6%)	97 (-4%)
		e2	99	94 (-5%)	89 (-10%)	91 (-8%)
		e3	97	88 (-9%)	84 (-14%)	86 (-12%)
7	2.75	e1	89	86 (-3%)	82 (-9%)	84 (-6%)
		e2	83	81 (-3%)	77 (-8%)	78 (-6%)
		e3	79	76 (-4%)	72 (-9%)	73 (-7%)

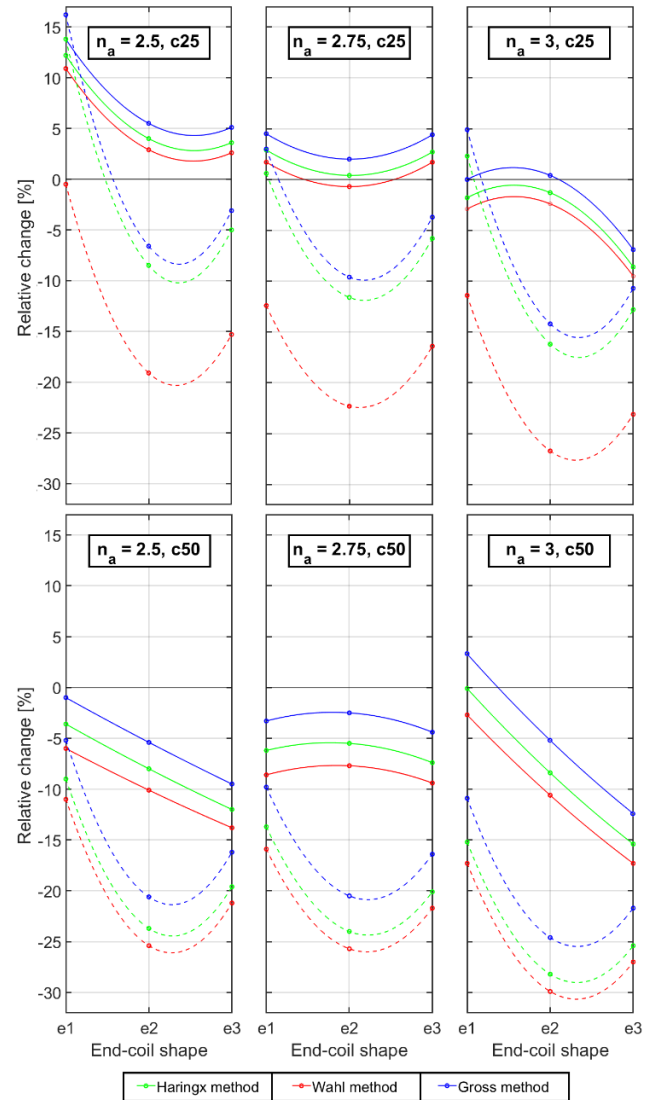


Fig. 3. Relative change between the stiffness values obtained from the experiments and the stiffness values calculated by the methods cited. Solid lines correspond to springs with index C = 7 and dashed lines to springs with index C = 5

This phenomenon is presented in Fig. 9, where an analysis of the effect of the design of the end-coils, the number of active coils and the compression value on the relative difference between the results of Eqs (2), (5) and (7) and the experimental results is presented. In most of the cases studied, the Gross method gives the closest results to the experimental results, but even for this method the discrepancies with the experimental results often exceed 20%. An increase in axial deflection is accompanied by an increase in the discrepancy between the formula results and the experimental results. This trend was confirmed by the results of additional tests on the transverse stiffness of springs with index C = 5, the number of active coils $n_a = 2.5$ and the end-coil design e1, e2, and e3 at 37.5% axial deflection. Due to the scope of this

work, the detailed results of these additional studies are not presented in this paper.

The analysis carried out showed that the effect of end-coil design on the discrepancy between formula results and experimental results is greatest for full ($n_a = 3$) or half ($n_a = 2.5$) number of active coils. In the case of springs with an intermediate number of coils ($n_a = 2.75$), this influence was the smallest, in particular for springs with $C = 7$. It can also be seen that the stiffnesses calculated using the Gross method are always the highest and the Wahl method the lowest. The Haringx method gives intermediate results.

4. CONCLUSIONS

This paper presents the results of transverse stiffness tests on cylindrical helical compression springs. Approximately 1,300 measurements were made with 18 springs differing in end-coil design, the number of active coils, and the spring index. An analysis of these results was carried out and compared with the results of computational models available in the literature. The analysis showed that the transverse stiffness of a cylindrical compression helical spring can show significant differences depending on the direction of the transverse force. In the cases studied, the largest difference between the maximum and minimum stiffness of a single spring reached a value of 26% of the average value of this stiffness. This phenomenon is not taken into account in the computational models present in the literature, which are based on the equivalent column concept, according to which the transverse stiffness of a spring does not depend on the direction of application of the transverse load.

A comparison of the average stiffnesses calculated from the experiments with the results of the calculation models available in the literature showed that the relative differences exceeded 25% in many cases. Under real-world conditions, a spring is generally loaded transversely in some fixed direction on which its transverse stiffness is, for example, the highest. Therefore, the differences between the stiffness calculated from one of the cited calculation methods and the actual spring stiffness may be even greater.

Axial deflection affects the actual number of active coils and thus changes the distribution of the spring's transverse stiffness. Therefore, the influence of the end-coil design on the nature of this distribution cannot be unambiguously determined. However, research has shown that the design of the end coils has the greatest effect on the average stiffness value for springs with a smaller index and, at the same time, a larger lead angle. It has been shown that the effect of the end coil design on the transverse stiffness is greater when the spring has a half or full number of active coils, but less for springs with an intermediate number of these coils.

Research also showed that fulfilling the condition defined in the EN 13906-1 standard for stable transverse operation of the spring does not guarantee such operation, and a new relation needs to be formulated, taking into account the influence of the end-coil design on the stability of the spring under transverse loading conditions.

This research showed that a detailed analysis must be performed during the design of a spring for a precise application. In the case of short springs, it is necessary to perform tests and determine the characteristics of the designed spring. The results of the transverse stiffness measurements presented in this paper

can serve as a benchmark for the validation of FEM numerical models.

REFERENCES

- Cieplik G, Wójcik K. Conditions for self-synchronization of inertial vibrators of vibratory conveyors in general motion. *Journal of Theoretical and Applied Mechanics*. 2020;58(2): 513–524. <https://doi.org/10.15632/jtam-pl/119023>
- Lee CM, Goverdovskiy VN. A multi-stage high-speed railroad vibration isolation system with 'negative' stiffness. *Journal of Sound and Vibration*. 2012;331(4): 914–921. <https://doi.org/10.1016/j.jsv.2011.09.014>
- Lu Z., Wang X., Yue K., Wei J., Yang Z. Coupling model and vibration simulations of railway vehicles and running gear bearings with multitype defects. *Mechanism and Machine Theory*. 2021;157: 104215. <https://doi.org/10.1016/j.mechmachtheory.2020.104215>
- Vazquez-Gonzalez B., Silva-Navarro G. Evaluation of the Autoparametric Pendulum Vibration Absorber for a Duffing System. *Shock and Vibration*. 2008;15(3–4): 355–368. <https://doi.org/10.1155/2008/827129>
- Yıldırım V. Exact Determination of the Global Tip Deflection of both Close-Coiled and Open-Coiled Cylindrical Helical Compression Springs having Arbitrary Doubly-Symmetric Cross-Sections. *International Journal of Mechanical Sciences*. 2016;115–116: 280–298. <https://doi.org/10.1016/j.ijmecsci.2016.06.022>
- Paredes M. Enhanced Formulae for Determining Both Free Length and Rate of Cylindrical Compression Springs. *Journal of Mechanical Design*. 2016;138(2): 021404. <https://doi.org/10.1115/1.4032094>
- Liu H., Kim D. Effects of end Coils on the Natural Frequency of Automotive Engine Valve Springs. *International Journal of Automotive Technology*. 2009;10(4): 413–420. <https://doi.org/10.1007/s12239-009-0047-8>
- Haringx J. A. On Highly Compressible Helical Springs and Rubber Rods, and their Application for Vibration-Free Mountings. *Philips research reports*. 1949;4: 49–80.
- Wittrick W. H. On Elastic Wave Propagation in Helical Springs. *International Journal of Mechanical Sciences*. 1966;8(1): 25–47. [https://doi.org/10.1016/0020-7403\(66\)90061-0](https://doi.org/10.1016/0020-7403(66)90061-0)
- Jiang W., Jones W. K., Wang T. L., Wu K. H. Free Vibration of Helical Springs. *Journal of Applied Mechanics*. 1991;58(1): 222–228. <https://doi.org/10.1115/1.2897154>
- Kobelev V. Effect of Static Axial Compression on the Natural Frequencies of Helical Springs. *Multidiscipline Modeling in Materials and Structures*. 2014;10: 379–398. <https://doi.org/10.1108/MMMS-12-2013-0078>
- Mottershead J. E. Finite Elements for Dynamical Analysis of Helical Rods. *International Journal of Mechanical Sciences*. 1980;22(5): 267–283. [https://doi.org/10.1016/0020-7403\(80\)90028-4](https://doi.org/10.1016/0020-7403(80)90028-4)
- Taktak M., Dammak F., Abid S., Haddar M. A Finite Element for Dynamic Analysis of a Cylindrical Isotropic Helical Spring. *Journal of Mechanics of Materials and Structures*. 2008;3(4): 641–658. <http://doi.org/10.2140/jomms.2008.3.641>
- Michalczyk K. Analysis of Lateral Vibrations of the Axially Loaded Helical Spring. *Journal of Theoretical and Applied Mechanics*. 2015;53(3): 745–755. <https://doi.org/10.15632/jtam-pl.53.3.745>
- Michalczyk K., Bera P. A Simple Formula for Predicting the First Natural Frequency of Transverse Vibrations of Axially Loaded Helical Springs. *Journal of Theoretical and Applied Mechanics*. 2019;57(3): 779–790. <https://doi.org/10.15632/jtam-pl/110243>
- Berger C., Kaiser B. Results of Very High Cycle Fatigue Tests on Helical Compression Springs. *International Journal of Fatigue*. 2006;28(11): 1658–1663. <https://doi.org/10.1016/j.ijfatigue.2006.02.046>
- Zhou C. et al. An Investigation of Abnormal Vibration – Induced Coil Spring Failure in Metro Vehicles. *Engineering Failure Analysis*. 2020;108: 104238. <https://doi.org/10.1016/j.engfailanal.2019.104238>

18. Sobaś M. Analysis of the Suspension of Freight Wagons Bogies Type Y25. *Pojazdy Szynowe*. 2014;3: 33–44.
19. Swacha P., Kotyk M., Ziółkowski W., Stachowiak R. Stand for testing the fatigue life of compression springs. *Developments in Mechanical Engineering*. 2021;17(9): 73–85.
<https://doi.org/10.37660/dme.2021.17.9.6>
20. Czaban J., Szpica D. The didactic stand to test of spring elements in vehicle suspension. *Acta Mechanica et Automatica*. 2009;3(1): 33–35.
21. Gross S. *Berechnung und Gestaltung von Metallfedern*, Springer-Verlag Berlin Heidelberg GmbH. 1951.
22. Wahl A. M. *Mechanical Springs*. Penton Publishing Company. 1944.

This work was supported by the AGH University of Science and Technology under research program No. 16.16.130.942.

Robert Baran:  <https://orcid.org/0000-0002-0711-230X>

Krzysztof Michalczyk:  <https://orcid.org/0000-0002-1024-5947>

Mariusz Warzecha:  <https://orcid.org/0000-0002-7417-1561>